DEVELOPMENT OF A NOVEL JOINT SYSTEM FOR MID-TO-HIGHRISE CLT WALL BUILDINGS IN SEISMIC REGIONS

World Conference on Timber Engineering Oslo 2023

DEVELOPMENT OF A NOVEL JOINT SYSTEM FOR MID-TO-HIGH-RISE CLT WALL BUILDINGS IN SEISMIC REGIONS

Ahmad Ghazi Aljuhmani[1], Eito Atsuzawa[2], Arata Minegishi[3], Kazuki Tsuda[4], Yutaka Goto[5], Masaki Maeda[6]

ABSTRACT: In Japan, the possibility of multi-story timber buildings is not yet practiced at a large scale due to the complex structural design process and construction cost. In conventional CLT buildings in Japan, a high number of complex steel connections are required. In this practice, complex processing of CLTs panel is also required. The objective of this paper is to propose easy-to-apply and easy-to-design steel joints. The proposed joint is designed to resist both shear and tensile forces to reduce complex steel parts. Single-bolt element tension tests were conducted to investigate the effect of the fibre direction, bolt diameter, and bolt embedded length. Cyclic loading for single and coupled CLT walls with the proposed joints was also conducted. The failure characteristics and strength of single-bolt connections could be predicted by the ratio of bolt embedded length and diameter. The fibre direction was found to have a minor effect on the connection strength. The proposed joint system showed high strength and ductility as found by the cyclic loading. The lateral strength of a wall with two panels was double the single wall case, indicating the lack of interaction between the two panels.

KEYWORDS: Cross-laminated Timber, Hybrid structure, Steel plate-bolt connections, Shear walls, Rocking walls

1 INTRODUCTION

Timber, as a construction material with its carbon-storing capability and renewability, can play an essential role in reducing GHGs emissions related to the construction sector. In Japan, although 66% of the total land area is covered by forests (Japanese Forestry Agency (JFA)), these renewable resources are not being used to their full potential. Buildings higher than three stories (mid-to-high-rise buildings) are mainly non-wooden structures [1], with a share of only 0.06% for timber buildings. This is attributed to the strict seismic and fire protection requirements. To overcome these challenges, Cross-laminated Timber (CLT) is considered a promising engineered wood product (EWP). When compared to sawn timber, CLT can secure the structural and fire safety requirements more efficiently. The laminated structure of CLT helps control the strength, reduces the effect of defects, and increases the dimensional stability of the element [2]. In Japan, the self-sufficiency rate of wood is only about 41%. The commonly used wood in Japan is cedar, which has relatively lower strength and larger number of knots and defects compared to other species. In addition, due to the high cost of timber production and inefficient forest management, imported timbers are more competitive in terms of cost and quality. Therefore, recently, the Japanese government has been putting many efforts to increase the use of domestic forest resources. For example, a law for promoting the use of timber in public buildings was enacted in 2010. By using CLT as a construction material, it is believed that we can ensure utilizing the domestic wood resources, as high strength of the CLT members can be achieved with relatively low-strength wood raw material.

In Japan, in order to fulfil the seismic requirements for the CLT walls, connections with high shear and tensile strength are generally required. However, in the common design practice for CLT buildings, an unreasonable amount of CLT walls (i.e., to compensate for the low strength and stiffness connections), and a large number of complex connections and CLT processing are needed.

In light of these problems, and in order to promote mid-to-high-rise CLT buildings, CLT-steel hybrid structures can be a possible solution. Combining CLT as a low carbon footprint material with a high strength-to-weight ratio with steel which has high ductility and recycling potential would result in a superior structural system in terms of structural performance (i.e., stiffness, strength, ductility, and energy dissipation) and environmental impact. The seismic behaviour of the structure using innovative CLT-steel hybrid systems was investigated by several researchers in the past years [3][7]. Kanazawa et al. [8] experimentally investigated the structural

[1] Ahmad Ghazi Aljuhmani, Tohoku University, Japan, aljehmani@rcl.archi.tohoku.ac.jp
[2] Eito Atsuzawa, Taisei Corporation, Japan, atzeit00@pub.taisei.co.jp
[3] Arata Minegishi, Tohoku University, Japan, minegishi@rcl.archi.tohoku.ac.jp
[4] Kazuki Tsuda, Tohoku University, Japan, tsuda@rcl.archi.tohoku.ac.jp
[5] Yutaka Goto, Chalmers University of Technology/Tohoku University, Sweden/Japan, yutaka@chalmers.se
[6] Masaki Maeda, Tohoku University, Japan, maeda@archi.tohoku.ac.jp

https://doi.org/10.52202/069179-0162

performance of several steel frames with CLT infill using small-diameter drift pin connections. They found that the use of CLT walls can increase the stiffness and strength by 1.5 to 2.3 times and 1.2 to 1.4 times, respectively, compared to the bare steel frame. In the previous studies, existing connection detail, such as tensile bolts, have been considered and the high strength and stiffness of CLT panels have not been fully utilized. Therefore, the objectives of this study are 1. Development of an easy-to-apply bolt-type steel joint system for CLT-steel hybrid buildings that can utilize the strength of CLT. 2. Experimentally investigate the structural performance of the bolted connection (i.e., strength, failure mechanism, and effect of fibre direction). 3. Experimentally investigate the structural performance of the proposed joint system by full-scale CLT wall-steel beam tests.

2 OUTLINE OF PROPOSED JOINT

In this research, a CLT wall-steel frame hybrid structural system was proposed, as shown in Figure 1. In this system, CLT walls are inserted into the steel frame to increase their seismic capacity. To connect the CLT wall with the steel beams of the structure, a joint system using bolted CLT connections was proposed and developed. The proposed joint system consists of four connections which are located at the four corners of the CLT panel, as shown in Figure 2.a. For each connection, a steel plate is connected to only one side of the CLT wall panel by large-diameter high-tensile bolts (HTBs), that work under shear (i.e., the HTBs resist the forces applied on them mainly by shear stresses only and not with friction stresses). Large-diameter bolts were used to achieve high strength and stiffness of the joint in order to utilize the structural advantages of CLT. The panels are then connected to the steel beam with these connections. Compared to the conventional connections (e.g., tensile bolts, Figure 2.b) the proposed joint system has the following advantages: 1. Relatively high stiffness and strength with a ductile behaviour are expected. 2. Resisting of bidirectional force that is resulted from shear and tension (uplift) forces induced by the horizontal load applied on the wall. 3. Simple connections with less complex CLT processing, such as cutting work, with high repairability of the damaged walls.

Under horizontal shear forces (Q) a moment is generated at the bottom of the wall ($M_{W\text{-}B}$). As shown in Figure 3, on the compression side of the wall, the bolts are assumed to resist only shear forces while the compression forces are resisted by the CLT wall. On the tension side of the wall, the bolts resist bidirectional forces of vertical forces (tension) and horizontal forces (shear). For each bolt, the resistance force of the bolt (P_θ, grey arrow in Figure 3) is a combination of vertical and horizontal forces, and thus it is tilted with an angle (θ). The shear and tensile strength of the connections are calculated by taking the result of P_θ on the vertical and horizontal axis multiplied by the number of bolts (n), as shown in Equations (*1*) and (*2*).

$$T_y = n \times P_\theta \times cos\theta \quad (1)$$

$$Q_y = n \times P_\theta \times sin\theta \quad (2)$$

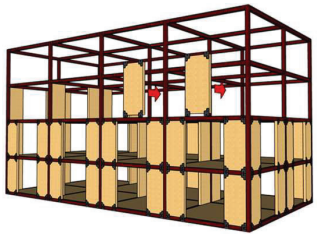

Figure 1: *Basic concept of the proposed CLT-steel hybrid structure*

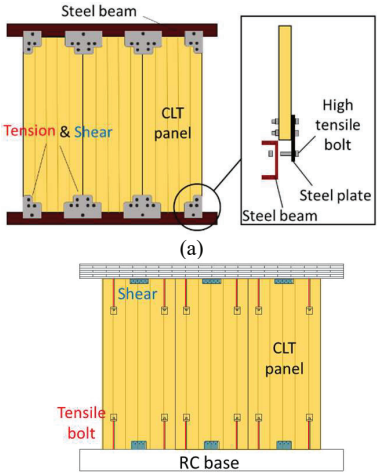

Figure 2: *Comparison between (a) the proposed joint system, and (b) the conventional connections system of CLT panels*

In the case of one-bolt connections, shear brittle failure or ductile embedment failure are considered possible failure modes, as shown in Figure 4. The type of failure can be controlled by changing the embedment length of the bolt (L_n) and the bolt diameter (Φ). The strength (P_θ) for each bolt is calculated as the minimum of CLT shear strength (Q_s) and CLT embedment strength (Q_{cv}), as (Equations (3)-(5)). The (L_n/Φ) ratio for the proposed joint is designed to have ductile embedment failure.

$$P_\theta = \min(Q_s, Q_{cv}) \quad (3)$$

$$Q_s = \tau \times 2 \times L_n \times t \quad (4)$$

$$Q_{cv} = \sigma_{cv} \times \phi \times t \quad (5)$$

Where τ and σ_{cv} (N/mm^2) are the shear and embedment strength of CLT, respectively. t (mm) is the thickness of CLT.

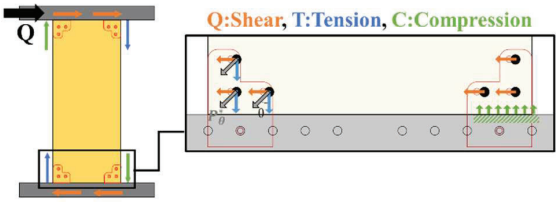

Figure 3: *Load transfer mechanism of the proposed joint system*

https://doi.org/10.52202/069179-0162

To calculate the yielding flexural moment capacity and rotation angle of the CLT wall, the following approach is used. In Japan, in CLT-panel system design practice, in order to ensure ductility, the strength of the wall is generally determined by the yielding of the tensile connections of the CLT wall panel. Minegishi et al. [9] proposed a method to calculate the bending moment capacity of the CLT wall in the same approach as calculating the bending moment of reinforced concrete columns. The calculation approach is illustrated in ***Figure 5***.a. The flexural yielding moment of the wall (M_y) is calculated by Equation (*6*). The shear strength of the wall at flexural yielding (Q_y) is calculated by Equation (7) using M_y. The yielding rotational angle of the wall (θ_y) and rotational stiffness (K_θ) is calculated by Equation (8) and (9), respectively. The neutral axial distance (x_n) is calculated using Equation (10) by taking the equilibrium of the compressive force of the CLT wall (C), the axial force (N), and the tensile yield force (T_y) (***Figure 5***.a.)

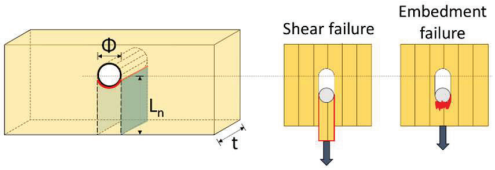

Figure 4: *Expected failure modes for one-bolt connection*

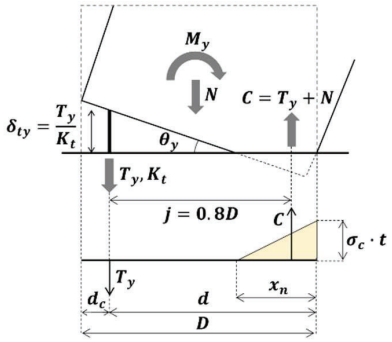

(a) allowable stress condition

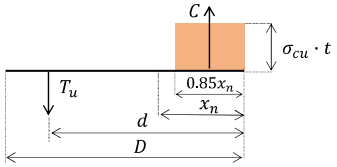

(b) ultimate state

Figure 5: *Stress condition of CLT wall, based on [9]*

$$M_y = T_y \times 0.8D + N \times 0.4D \quad (6)$$

$$Q_y = M_y/h \quad (7)$$

$$\theta_y = \delta_{ty}/(d - x_n) \quad (8)$$

$$K_\theta = M_y/\theta_y \quad (9)$$

$$x_n = 2(N + T_y)/\sigma_c t \quad (10)$$

Where D and t (mm) are the width and thickness of the wall, respectively. h (mm) is the inflection point height, and δ_{ty} (mm) is the deformation of the tensile connection. d (mm) and x_n (mm) are the distance from the tensile connection and neutral axis to the compression edge of the wall, respectively. σ_c (N/mm^2) is the allowable compressive strength of the CLT and it is equal to two-thirds of the compressive strength of CLT.

3 SINGLE-BOLT CONNECTION TEST

3.1 MATERIAL PROPERTIES

Material tests were conducted to get the embedment and shear strength of CLT based on the testing procedures mentioned in [10]. The tested CLT panels were five-layer 150 mm thick, made from Japanese cedar with Mx-60-5-5 (5-ply 5-layer) grade and composition [11]. The average CLT density was 400 kg/m^3, and the average moisture content was 12.0%. Three identical specimens were used for each material test, and the results are summarized in Table 1.

Table 1: *Results of the CLT material tests for single-bolt connection specimens*

Strength (MPa)	Shear		Embedment	
	Major	Minor	Major	Minor
	3.2	2.9	18.6	15.9

3.2 TEST MATRIX

In this study, component-level tests on double plate one-bolt connections were conducted (i.e., two steel plates on both sides of the CLT panel were fixed with a HTB). All the tested specimens have the same dimensions as shown in Figure 6 and were tested under monotonic loading. the tested specimens are summarised in Table 2. In order to investigate the effect of the embedment length (L_n) on the failure mode (as explained in section 2), the experimental parameter was the (L_n/Φ) ratio. In addition, to investigate the effect of fibre angle (i.e., loading direction) on the load-bearing capacity, the outer layer fibre direction (θ) was taken as another parameter. A bolt with a diameter of Φ=40 mm was installed into the specimens. For each type of specimen, three replicates were tested.

3.3 LOADING SET-UP

The loading set-up of the tested specimens is shown in Figure 7. The CLT panel was fixed on top of two steel bases with two threaded rods at each side to prevent out-of-plane deformation. A single 300 kN jack was used to apply a monotonic downward force on the connection's steel bolt, and the loading rate was in the range of 0.15–0.2 mm/s. The vertical displacement of the bolt was taken as the average value of two LVDTs that were attached on both sides of the specimen.

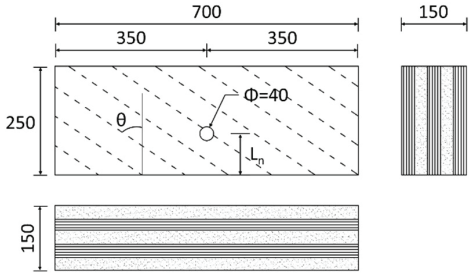

Figure 6: *Dimensions of the tested specimens (mm)*

https://doi.org/10.52202/069179-0162

Table 2: *Test matrix of the CLT panels*

Specimen name	Panel thickness [t] (mm)	Bolt diameter [Φ] (mm)	Embedment length [L_n] (mm)	Fiber angle [θ] (°)	$L_n/Φ$	No. of specimens
40-0-50				0		
40-30-50				30		
40-45-50	150	40	150	45	1.3	3
40-60-50				60		
40-90-50				90		
40-0-100				0		
40-30-100				30		
40-45-100	150	40	150	45	1.3	3
40-60-100				60		
40-90-100				90		
40-0-150				0		
40-30-150				30		
40-45-150	150	40	150	45	1.3	3
40-60-150				60		
40-90-150				90		

3.4 TEST RESULTS

The relation between $L_n/Φ$ ratio and the load-bearing capacity of the tested specimens and fibre direction angle (θ=0° and θ=90°) is shown in Figure 8. All specimens with $L_n/Φ$=1.3 had a shear failure with the lowest load-carrying capacity. Most of the specimens with $L_n/Φ$=3.8 showed ductile embedment failure. For specimens with $L_n/Φ$=2.5, about half of the specimens showed bearing failure, and shear failure was observed for the other half. A comparison between the experimental results and the calculation methods explained in section 2 is shown in Figure 8. The calculated values have a similar tendency to the experimental values and are generally conservative (lower) than experimental values. The failure mechanism can be predicted, and the connection can be designed to have ductile embedment failure by designing $L_n/Φ$ ratio. The load-bearing capacity of a one-bolt connection can be roughly estimated by equations (4) and (5). As shown in Figure 9, the maximum strength obtained from the tests is almost the same regardless of the fibre direction angle (θ). It can be said that the influence of (θ) is almost negligible.

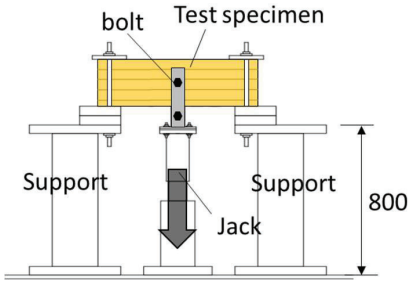

Figure 7: *Loading set-up for single drift pin test*

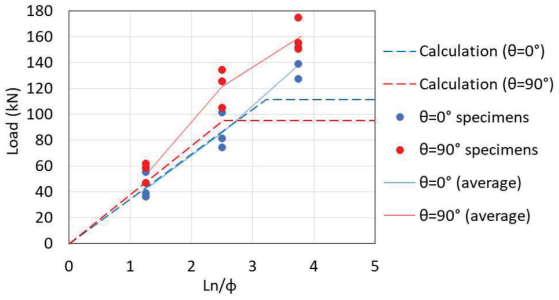

Figure 8: *Effect of Ln/Φ ratio on the load-carrying capacity*

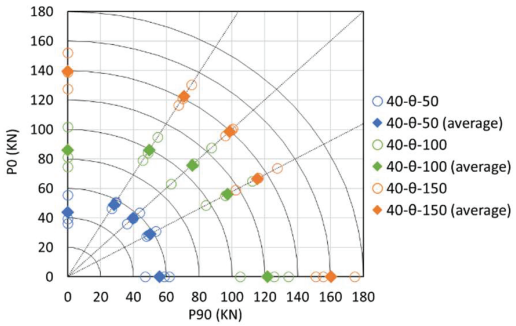

Figure 9: *Effect of loading angle relative to CLT fibre direction on the strength of the drift pin*

4 SHEAR WALLS TESTS

4.1 MATERIAL PROPERTIES

In order to investigate the structural performance of the proposed hybrid structural system, quasi-static cyclic loading tests on three different CLT wall-steel beam specimens were conducted. 90 mm thick CLT panels made from Japanese cedar with Mx-60-3-3 (3-ply 3-layer) grade and composition [11] were used for shear wall tests. The average CLT density was 393 kg/m^3, and the average moisture content was 12.2%. Material tests were conducted to obtain compression, embedment, and shear strength of CLT based on the testing procedures mentioned in [10]. Three identical specimens were used for each material test, and the results are summarized in Table 3.

Table 3: *Results of the CLT material tests for CLT wall tests*

	Compression		Shear		Embedment	
Strength (MPa)	Major	Minor	Major	Minor	Major	Minor
	23.7	10.9	3.8	2.6	21.6	15.5
	Compression [E]		Shear [G]		Embedment stiffness	
Modulus (MPa)	Major	Minor	Major	Minor	Major	Minor
	5926.9	2322.5	299.5	199.2	1767.2	1188.9

4.2 TEST MATRIX

Three CLT wall-steel beam specimens with different connections and wall configurations were tested. The details of the specimens are shown in Table 4. For all tests, 90-mm thick, 1000 mm by 2400 mm CLT wall panels were used. For the steel beams, two-meter C-section steel beams (200 × 90 × 8 × 13.5 in the Japanese Industrial Standards (JIS G 3192)) were attached to the top and bottom of the wall. One of the specimens contained a single CLT wall with the proposed bolt connection (SSB). The second specimen consisted of two CLT wall panels connected in plain using the proposed joint (SCB). SCB wall specimen was tested to investigate the coupled-wall behaviour of the proposed joint system. The third specimen (SSS) is identical to specimen SSB except for the CLT wall-to-beam connections. In the SSS specimen, conventional screw connections were used (i.e., steel plate fixed to one side of the wall using self-tapping screws). The details and dimensions of the connections are shown in Figure 9. 9-mm thick steel plate was used for all the connections. For the bolt connections, three 20-mm HTBs were used, and ($L_n/Φ$) ratio was chosen as $L_n/Φ$=3.5 to

https://doi.org/10.52202/069179-0162

ensure the targeted embedment failure. For screw connections, STS C65 screws with 5.5 kN strength were used, according to the Japanese CLT Design Manual [11]. The number of screws (9) was chosen so that the load-bearing capacity of the conventional connection is equal to that of the bolt connection. The CLT wall was connected to the steel beam using 24-mm HTBs.

4.3 LOADING SET-UP

The CLT wall specimens were tested under quasi-static cyclic loading with the set-up shown in Figure 11. The specimens were loaded by two 200 kN centre-hole jacks at each side of the specimen (pull forces were applied). The two jacks were connected to the steel beams using wire ropes, and a pre-tension force of 10 kN was applied to the two wire ropes in order to prevent the twisting of the specimen in the out-of-plane direction. No axial load was applied to the wall; however, four tie bars were attached to the top steel beam as an uplifting constraint. each tie bar was pre-stressed with a 5 kN tensile force. The lateral load was applied as an incremental cyclic loading based on the loading protocol provided in [12]. Three cycles for each peak drift were adopted.

Table 4: *Test matrix of the CLT wall tests*

Specimen name	SSB	SCB	SSS
	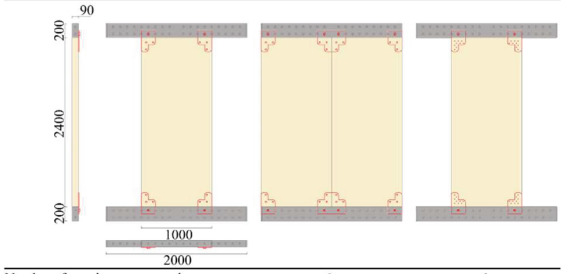		
Number of panels	1	2	1
Connection type	Bolt (HTB)	Bolt (HTB)	Screws (STS · C65)
Bolts/screws diameter (mm)	20	20	6.5
No. of bolts/screws	3	3x2 (6)	9

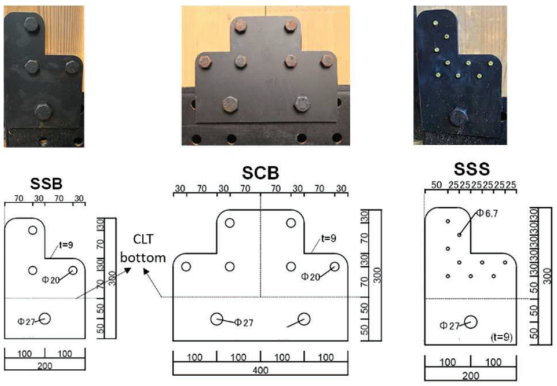

Figure 10: *Details of the steel plates used in the connections*

4.4 INSTRUMENTATION

The applied lateral load was measured using a centre-hole load cell. A typical instrumentation layout for the CLT wall tests is shown in Figure 12. LVDT sensors were attached to the tested specimens to measure story drift, and the story drift angle was calculated by considering the story height between the middle of the top and bottom beam (i.e., calculated by dividing the lateral load by the story height (2600 mm)). Rocking, sliding, shear, and bending deformation of the CLT wall panel were also measured. LVDT sensors to measure the neutral axis of the wall were also attached to the top and bottom of the wall. In addition, to calculate the axial forces in the tie bars, strain gauges were attached to all the bars. The axial force of the tie bar can be calculated as shown in Equation (11). The flexural moment in the bottom of the CLT wall ($M_{W\text{-}B}$) is then calculated using Equation (12) by subtracting the moment caused by the tie bar M_r from the moment of the entire system (M_{total}).

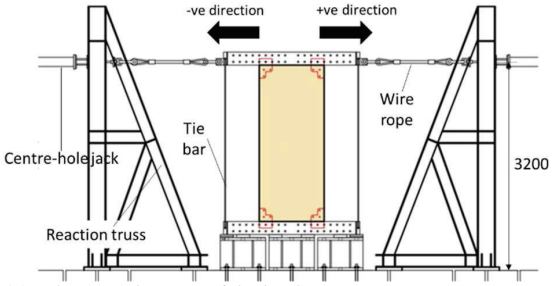

(a) Schematic diagram of the loading set-up

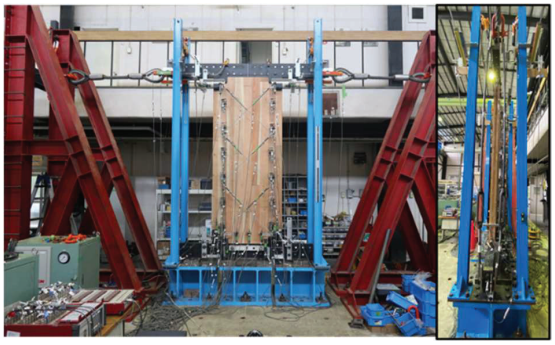

(b) Photo of the loading set-up

Figure 11: Loading set-up of shear wall tests

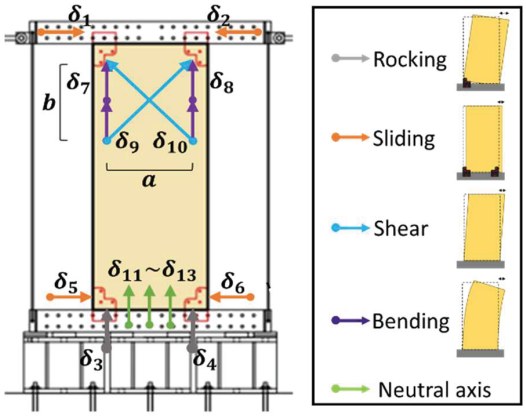

Figure 12: *An example of single wall (SSB) instrumentation*

https://doi.org/10.52202/069179-0162

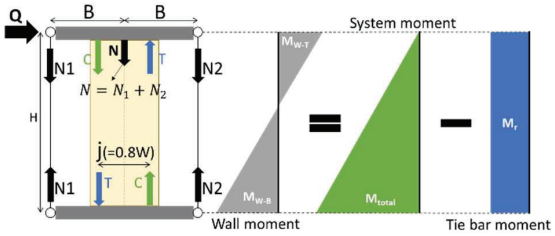

Figure 13: *Calculation method of the wall moment*

$$N_i = \varepsilon \times E \times A \quad (11)$$

Where ε (mm/mm) is the strain of the tie bar as measured, E (N/mm^2) is Young's modulus of the steel bar (2.05×10^5 N/mm^2), and A (mm) is the cross-sectional area of the tie bar (478.8 mm^2).

$$M_{W-B} = M_{total} - M_r \quad (12)$$
$$M_{total} = Q \times H \quad (13)$$
$$M_r = (N_1 - N_2) \times B \quad (14)$$
$$T = M_{wb}/j - 0.5N \quad (15)$$

Where H (mm) is the story height (2600 mm), N_1 and N_2 (kN) are the axial forces in the left and right tie bars, respectively. B (m) is the distance between the tie bar and the centre of the wall (1.025 m). N (kN) is the axial force applied to the wall and is equal to N_1+N_2. j (m) is the distance between the two connections at the bottom of the wall (0.8×D (1.2) =0.96 m), as explained in section 2.

4.5 RESULTS AND DISCUSSION

4.5.1 Failure characteristics

Photos of the failed single wall and coupled wall specimens (SSB and SCB, respectively) are shown in Figure 14. For the SSB specimen, at the bottom tensile connection, the outer layer of the wall (i.e., the outer lamina) failed in plug shear-out failure at 1% story drift angle. After that, a decrease in stiffness was observed; however, the load-bearing capacity of the wall continued to increase. This increase can be attributed to the effect of the compression strut inside the CLT wall, which appears as compression stresses at the compression side of the top and bottom part of the wall. At 5% story drift, the steel beam yielded in flexure (Figure 14.a), and the loading was terminated. For the SCB specimen, the outer lamina of the CLT wall at the tensile connection had a plug shear-out failure at 1.3% story drift. The load-bearing capacity continued to increase after the shear failure. At 4.8% story drift, the tensile connection in the middle of the wall had block shear failure, as shown in Figure 14.b, and the loading was terminated at 5% story drift. For the single wall with screw connections specimen (SSS), at 3% story drift, the screws of the bottom tensile connection started to fracture (2 screws). At 3.7% story drift, a large number of screws in the top and bottom tensile connections were broken and the test was terminated.

Although the expected failure type was supposed to be a uniform embedment failure, the bolt was tilted to the steel plate side of the CLT panel during the experiment. This failure mode was not considered in the design of the connections. In Europe, to calculate the load-bearing capacity of one-bolt connections for ductile failure the European yield model (EYM) is used. Using EYM the strength and failure mode of the connection are mainly governed by the bolt diameter to CLT panel's thickness ratio (Φ/t). When the EYM was applied to the connection used in this test, it was found that the expected failure is bolt-yielding failure (mode 2, Φ/t= 0.22), as shown in Figure 15. The ductile failure strength of the proposed joint was calculated based on the EYM equations provided in [13] and was compared to the experimental results. In order to apply the EYM to CLT, the average embedment strength across the width of the CLT panel was used, instead of lamella-by-lamella calculation. The values of the embedment strength of CLT provided in section 4.1 were used.

(a) SSB specimen

(b) SCB specimen

Figure 14: Failure characteristics of the tested specimens

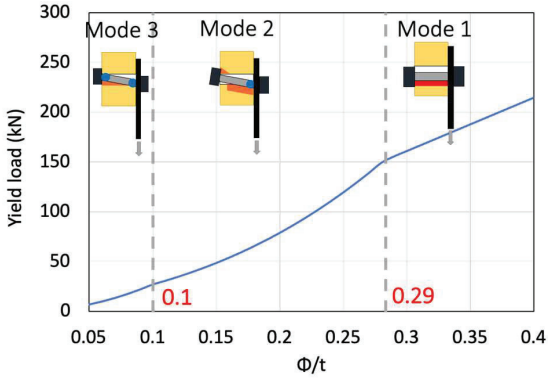

Figure 15: *Failure modes based on the EYM [13]*

4.5.2 Load-deformation response

The shear force-story drift curve for the SSB specimen is shown in Figure 16. The difference between maximum strength in the positive and negative direction was within 8%. When compared to calculation values based on uniform embedment failure (as explained in section 2), the experimental maximum strength (P_{max}) was 38% smaller. However, when compared to strength derived from the EYM, the experimental maximum strength was 18% larger. The EYM model can predict the load-bearing capacity of the proposed joint system with an acceptable accuracy. In addition to that, it was found that high shear strength per wall (τ=0.84 MPa) can be achieved, compared to 0.15 MPa for the wall with a conventional tensile bolt connection. This value (0.15 MPa) is calculated based on the standard strength of the CLT wall used in the simplified design method that is provided in the Japanese CLT Design Manual [11].

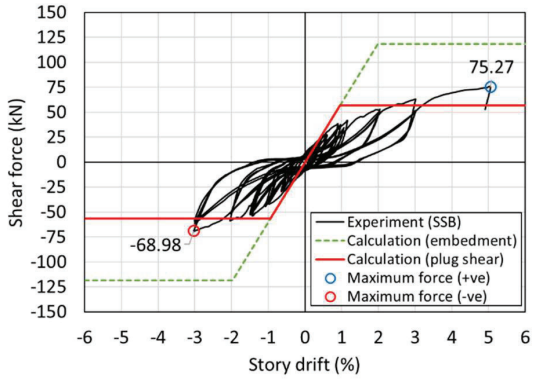

Figure 16: *Shear force-story drift curve for SSB wall specimen*

The shear force-story drift curve for the SSS specimen is shown in Figure 17. The maximum strength in the positive direction was 23% higher than that for the negative direction. Although the screw connection was designed to have a similar strength capacity to the bolt connection, the maximum strength of the SSS specimen was 32% smaller. The shear force-story drift curve for the SCB specimen is shown in Figure 18. The difference between maximum strength in the positive and negative direction was also within 8%. When compared to the single wall specimen (SSB), the maximum strength of the SCB specimen was only two times larger (198%). Therefore, each wall behaved as a separate wall and the proposed connections need to be improved to ensure the single-panel rocking behaviour.

The bilinear curves and the characteristic values (i.e., initial stiffness (K), yield strength (P_y), ultimate strength (P_u), and ductility (μ)) of the tested specimens were calculated based on the standard method described in the Japanese CLT Design Manual [11]. This method is based on the method proposed by Yasumura [14] for framed shear walls subjected to lateral load and is illustrated in Figure 19. The characteristic values of the tested specimens are summarised in Table 5. As a general tendency, for all the characteristic values, the single wall with screws connections specimen (SSS) had smaller values than the single wall with bolted connections specimen (SSB), as shown in Figure 20.a. The SSS specimen had a 60% smaller initial stiffness than the SSB specimen. When compared to the single wall specimen (SSB), the characteristic values of the coupled wall specimen (SCB) were almost two times larger on average. The initial stiffness of the SCB specimen was only 25% larger than the SSB specimen.

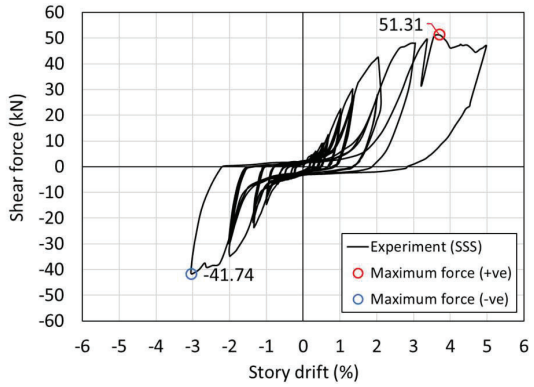

Figure 17: *Shear force-story drift curve for SSS wall specimen*

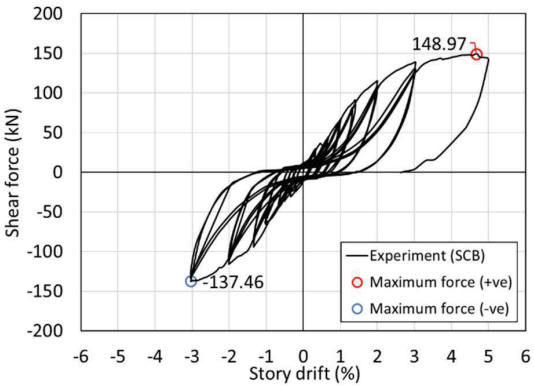

Figure 18: *Shear force-story drift curve for SCB wall specimen*

https://doi.org/10.52202/069179-0162

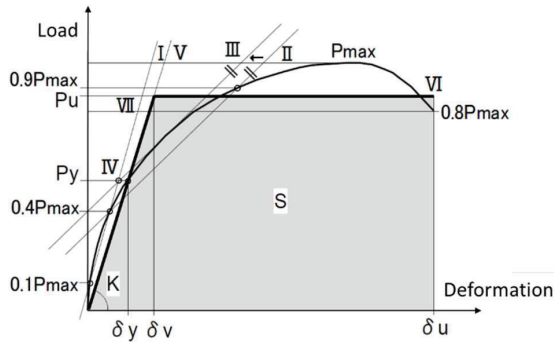

Figure 19: *Calculation method of bilinear of test load-deformation curves, as derived from [11]*

Table 5: *Summary of the characteristic values for specimens*

Specimen	Max. strength P_{max} (kN)	Yield strength P_y (kN)	Ultimate strength Pu (kN)	Initial stiffness K (kN/mm)	Ductility μ=δu/δv
SSB	75.3	40.6	65.6	1.4	2.7
SCB	149.0	97.1	140.2	2.4	2.2
SSS	51.3	37.7	46.1	0.8	2.3

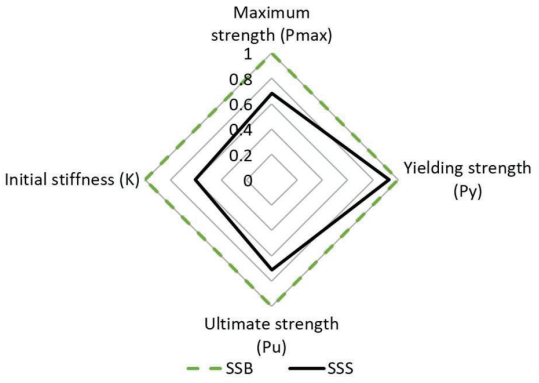

(a) bolts single wall (SSB) vs. screws single wall (SSS)

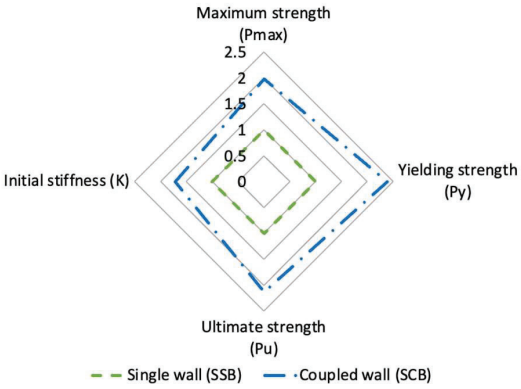

(b) single wall (SSB) vs. coupled wall (SCB)

Figure 20: *Comparison of the characteristic values for the tested wall specimens*

4.5.3 Performance of the proposed joint system

In this section, the performance of the proposed connection, as observed in the single wall specimen (SSB), is discussed. The contribution ratios of the different deformation components for the CLT wall panel at each peak drift in the positive direction are illustrated in Figure 21. In Figure 21, the contribution of the connection to the total deformation, and the bending and shear deformation of the wall panel are compared to the story drift. Deformation at the connection (rocking and sliding) was larger than the deformation of the CLT panel and was dominant from the small to ultimate story drift angle. Rocking deformation had the largest share with a 55.1% ratio on average, compared to the summation of the four components. The sliding deformation ratio was 32.5% on average. The CLT panel bending, and shear deformation ratio was 2.8% and 9.6%, respectively. It was found that the major component in the overall deformation of the wall is the rocking deformation, which represents the vertical deformation of the steel connection. This dominant rocking deformation was further investigated by looking into the relation between the moment at the bottom of the wall and the rocking angle of the wall, as shown in Figure 22.

In Figure 22, for experimental values, the rocking angle was taken as the value of the vertical LVDT sensors attached to the connection (δ_3 in Figure 12), and the flexural moment at the bottom of the wall ($M_{W\text{-}B}$) was calculated using the calculation method explained in section 4.4 (using Equation ((12)). To draw the calculation values curve, the rocking angle was calculated by the calculation method introduced in section 2 (using Equation (8)). Wall moment ($M_{W\text{-}B}$) was also calculated by the calculation method introduced in section 2. The calculated maximum moment was 16% smaller than the experimental result. The same tendency between calculation and experimental results was also found for the overall wall shear force-story drift. It was found that the introduced calculation method can be used to predict the structural behaviour of the proposed connection.

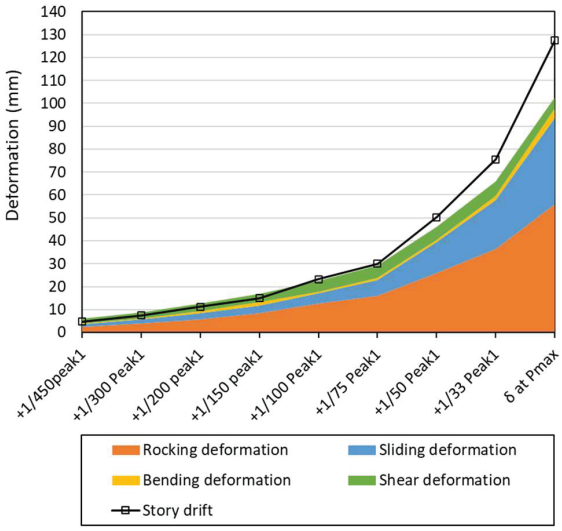

Figure 21: *Deformation components of single wall specimen (SSB) compared to the story drift (in positive direction)*

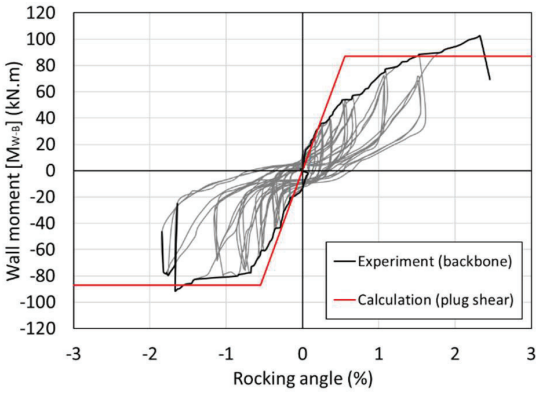

Figure 22: *Moment-rocking deformation curve of (SSB) wall*

5 CONCLUSIONS

In this paper, a novel steel joint system for CLT-steel hybrid structures in seismic regions was proposed. The connections used in this joint system consist of steel bolts and a steel plate and works under bi-directional loading condition. One-bolt connection tests were conducted to investigate the effect of loading direction. Also, full-scale CLT wall-steel beam cyclic tests were conducted to investigate the structural performance of the hybrid structural system. The findings of this research are as follows:

1. Simple and easy-to-install bolted connection that can utilize the actual strength of CLT was developed.
2. Based on the one-bolt connection tests, it was found that maximum strength can be predicted, and the connection can be designed to have ductile embedment failure with the considerable selection of the embedment length over bolt diameter ratio (i.e., L_n/Φ larger than 3.2). Also, for CLT panels with a one-bolt connection, the effect of loading direction on the ultimate strength was not significant (within 16%)
3. For CLT walls tests, the wall with the proposed joint system showed higher average shear strength of 0.83 MPa, compared to 0.15 MPa of conventional tensile bolt connection. The wall also showed ductile behaviour and did not fail until a large story drift angle of 5% (the story drift angle at steel beam yielding). Regarding the coupled wall test, the two walls behaved as separate single walls and the strength was about twice the single wall. Further improvements are required to secure the single-panel rocking behaviour.
4. In the wall-beam system, the deformation of the proposed connection was dominant (i.e., rocking 55.1% and sliding 32.5% of the wall lateral deformation). The proposed calculation method can be used to predict the performance of the joint system.

For future consideration, improvements of the proposed connection to ensure CLT embedment failure is needed. Also, further considerations to improve the rocking behaviour of the coupled walls are desirable.

ACKNOWLEDGEMENT

This research was supported by JSPS Kakenhi Grant Number JP19K22001, and by Miyagi Prefecture CLT Promotion Council. This fund is gratefully acknowledged. The support of Dr. Naoyuki Matsumoto, Assistant Professor, Tohoku University is also appreciated.

REFERENCES

[1] Japanese Forestry Agency, accessed 25 January 2023,<https://www.rinya.maff.go.jp/j/kikaku/hakusyo/r1hakusyo_h/all/chap3_2_2.html>. (In Japanese)
[2] Brandner R., Flatscher G., Ringhofer A., Schickhofer G., Thiel A.: Cross laminated timber (CLT): overview and development. European Journal of Wood and Wood Products, 74:331-351, 2016.
[3] Loss C., Rossi S., Tannert T.: In-plane stiffness of hybrid steel–cross-laminated timber floor diaphragms. Journal of Structural Engineering, 144(8):04018128, 2018.
[4] Khajehpour M., Pan Y., Tannert T.: Seismic Analysis of hybrid steel moment frame CLT shear walls structures. Journal of Performance of Constructed Facilities, 35(5):04021059, 2021.
[5] Dickof C., Stiemer S.F., Bezabeh M.A., Tesfamariam S.: CLT–steel hybrid system: Ductility and overstrength values based on static pushover analysis. Journal of Performance of Constructed Facilities, 28(6):A4014012, 2014.
[6] Bezabeh M.A., Tesfamariam S., Popovski M., Goda K., Stiemer S.F.: Seismic base shear modification factors for timber-steel hybrid structure: collapse risk assessment approach. Journal of Structural Engineering, 143(10):04017136, 2017.
[7] Tesfamariam S., Stiemer S.F., Dickof C., Bezabeh M.A.: Seismic vulnerability assessment of hybrid steel-timber structure: Steel moment-resisting frames with CLT infill. Journal of Earthquake Engineering, 18(6):929-944, 2014.
[8] Kanazawa K., Isoda H., Kitamori A., Usami T., Araki Y.: Structural performance of composite structure with CLT wall infilled in steel frames using drift-pin with steel plate. Journal of Structural and Construction Engineering, 86(788):1430-1439, 2021. (In Japanese)
[9] Minegishi A., Atsuzawa E., Maeda M.: Study on development of a simple and practical analytical model for structural design of CLT buildings. In: Proceedings of Annual Meeting Architectural Institute of Japan (AIJ), No.22246-22247:491-494, 2021. (In Japanese)
[10] Test Manual for Structural Timber Strength. Japan Housing and Wood Technology Center, 2011. (In Japanese)
[11] CLT Building Design Manual. Japan Housing and Wood Technology Centre, 2016. (In Japanese)
[12] JIS A 1414-2: Performance test methods of panel components for building construction. Japanese Standards Association, 2010. (In Japanese)
[13] AIJ Standard for Structural Design of Timber Structures. Architectural Institute of Japan, 2006. (In Japanese)
[14] Yasumura M.: Evaluation of wood framed shear walls subjected to lateral load. In: Proceedings of the 30th CIB-W18, Vancouver, Canada, 1997.

https://doi.org/10.52202/069179-0162